

Local coordination geometry around Cu^+ and Cu^{2+} ions in silicate glasses: an X-ray absorption near edge structure investigation

C. Maurizio¹, F. d'Acapito^{2,a}, M. Benfatto^{3,4}, S. Mobilio^{4,5}, E. Cattaruzza⁶, and F. Gonella¹

¹ INFN, Dipartimento di Fisica, Università di Padova, Via Marzolo 8, 35131 Padova, Italy

² INFN Grenoble Operative Group c/o European Synchrotron Radiation Facility, GILDA CRG, BP 220, 38043 Grenoble, France

³ European Synchrotron Radiation Facility, BP 220, 38043 Grenoble, France

⁴ Istituto Nazionale di Fisica Nucleare, Laboratori Nazionali di Frascati, P.O. Box 13, 00044 Frascati, Italy

⁵ Università "Roma Tre", Dipartimento di Fisica, Via della Vasca Navale 84, 00146 Roma, Italy

⁶ INFN, Dipartimento di Chimica Fisica, Università di Venezia, Dorsoduro 2137, 30123 Venezia, Italy

Received 30 April 1999

Abstract. We present an X-ray absorption near edge structure (XANES) study on Cu^+ and Cu^{2+} ions in silicate glasses at the Cu K-edge, aimed to determine the geometry of the local structure around the metal. This study is based on the comparison between experimental data and theoretical calculations made in the framework of multiple scattering theory. The XANES signals relative to several clusters are simulated on the basis of known crystalline structures involving Cu^+ and Cu^{2+} ions in silicate matrices. Concerning the Cu^{2+} in glass, the simulations suggest the presence of a square coordination of oxygen atoms around the absorber, with a possible presence of metal ions in the second shell. As for the Cu^+ ions, the metal clustering is excluded and a linear O–Cu–O coordination is evidenced.

PACS. 61.10.Ht X-ray absorption spectroscopy: EXAFS, NEXAFS, XANES, etc. – 61.43.Fs Glasses – 85.40.Ry Impurity doping, diffusion and ion implantation technology

1 Introduction

Copper-doped glasses are interesting materials in many respects. For instance, planar optical waveguides are obtained by doping surface layers of glass slides with metal ions *via* binary ion exchange [1]. Moreover, optical switching devices can be designed by exploiting composite systems consisting of metallic clusters embedded in glass [2]. These materials exhibit remarkable optical nonlinear response, with intensity-dependent index of refraction values up to 10^{-9} cm²/W, *i.e.*, 10^7 times higher than that of pure silica [3]. Copper-containing waveguides have also recently drawn new attention owing to their blue-green luminescence [4] properties.

Local atomic order plays a fundamental role in determining the optical response of copper-doped glasses. In particular, different coordination states of Cu^+ ions in glasses were found to be responsible for different luminescence emission and excitation properties [5]. For this reason, it is crucial to provide a full geometrical description of the first coordination shells around the metallic ion. We present here a detailed study of the local

structure around Cu^+ and Cu^{2+} ions dispersed in glassy model samples, obtained by either ion implantation or binary ion exchange, using X-ray near edge structure (XANES) [6] spectroscopy.

2 Experimental procedure

Model samples containing Cu^+ or Cu^{2+} ions prepared by either binary Cu^+ – Na^+ ion exchange or ion implantation were used. The ion exchanged soda-lime glass (sample E) was treated for 20 minutes in a molten eutectic bath of $\text{CuSO}_4:\text{Na}_2\text{SO}_4$ salts at 585 °C. Two other samples were obtained by ion implantation with Cu^+ ions at 160 keV to a fluency of 1×10^{16} ions/cm² of a soda-lime slide (sample IG) and a pure silica slide (sample IS). Cu K-edge X-ray absorption measurements were performed at the European synchrotron radiation facility (ESRF) on the bending magnet GILDA beamline. The monochromator was equipped with a couple of Si(311) crystals and ran in dynamical focusing mode [7], with an estimated energy resolution of about 0.3 eV. Harmonic rejection was achieved using a pair of Pd-coated mirrors with a cut-off energy of 21 keV. Spectra were collected at 77 K in

^a e-mail: dacapito@esrf.fr

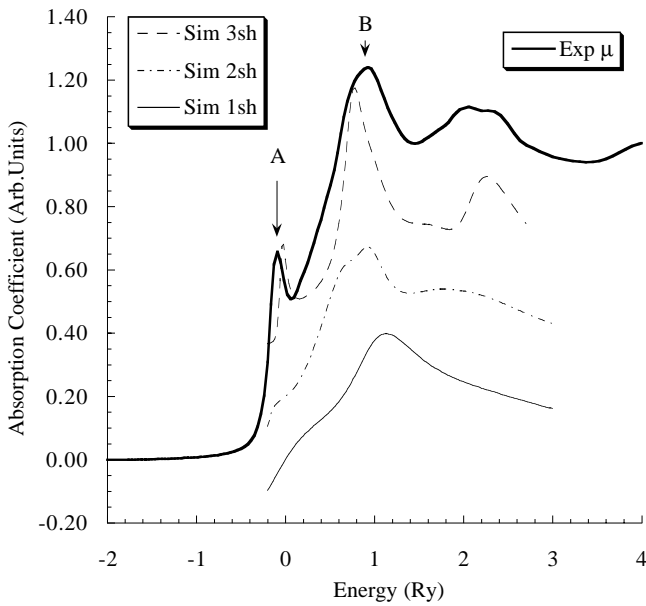


Fig. 1. Simulation with X- α potential of the Cu-K absorption edge of Cu_2O with 1 to 3-shell model clusters. The local cluster is made up of a first shell of two O atoms at 1.848 Å, then twelve Cu atoms at 3.019 Å and six O atoms at 3.540 Å.

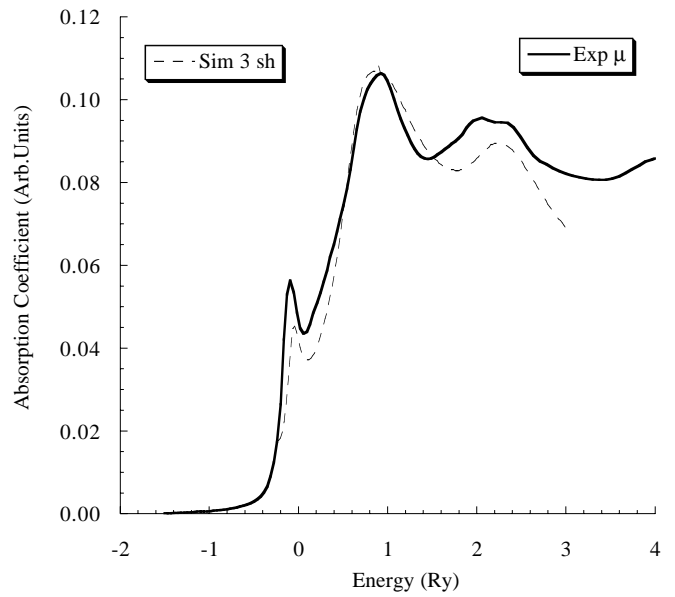


Fig. 2. Comparison between the experimental spectrum of Cu_2O and the 3-shell simulation using the Hedin-Lunqvist potential.

fluorescence mode using a Si PIN photodiode. Reference spectra were also collected at 77 K in transmission mode on Cu_2O and CuO crystalline powders deposited on millipore membranes. All the experimental XANES spectra were subtracted by a linear pre-edge background, normalizing the jump to 1 at 9600 eV. This point was chosen in a region where the amplitude of the EXAFS oscillations was much smaller than the atomic absorption jump. Energy scale was calibrated by putting the first inflection point of the edge spectrum of metallic Cu at 8979.0 eV.

3 XANES data analysis

Previous structural investigations [8] indicate that the geometry of the atomic environment of Cu ions strongly depends on the ion valence state. Cu^+ ion is known to usually form a collinear geometrical coordination with oxygen atoms, while Cu^{2+} coordinates oxygens in an octahedral-like geometry. Normally the octahedron is tetragonally distorted with an elongation of the bonds along the z -axis. Tetrahedral coordination around Cu^+ is present in its halides [9], while this coordination is not observed for Cu^{2+} . A comprehensive review on the coordination geometries of Cu ions can be found in reference [10]. Theoretical calculations of XANES spectra were made on the basis of multiple scattering formalism, using the CONTINUUM package developed at the INFN Laboratori Nazionali di Frascati [11,12]. The Coulomb part of the potential is built by superimposing the atomic charge densities obtained from Clementi-Roetti tables. The $Z+1$ approximation was used to account for the core-hole relaxation. Muffin-Tin radii were chosen according to the Norman criterion [13], and a 10% overlap was allowed

between contiguous spheres. For the exchange correlation part of the potential, we used the complex Hedin-Lunqvist (HL) self-energy, whose imaginary part accounts for the amplitude attenuation of the excited photoelectron due to the extrinsic losses. The calculated spectra are further convoluted with a Lorentzian curve to account for the core-hole lifetime (1.55 eV for the Cu K-edge [14]) and the energy resolution of the monochromator (0.3 eV using Si(311) crystals).

Our XANES simulation starts with the calculation of Cu K-edges of well-known crystalline structures as Cu_2O for Cu^+ and CuO for Cu^{2+} , to optimize the parameters of the calculation and understand the origin of the various features present in the experimental data. In Figure 1, we report the comparison of experimental data of Cu K-edge on crystalline Cu_2O [9] (solid line) with three calculations based on clusters made of 1, 2 and 3 shells, respectively. The X- α potential was used in this case. The XANES spectrum of crystalline Cu_2O is characterized by the presence of two peaks, one on the rising edge (peak “A”) at 8982 eV and a white line (peak “B”) at 8996 eV (Fig. 1). The “A” feature at 8982 eV is present in a number of Cu^+ compounds, and is particularly evident in linearly 2-coordinated systems [10]. It appears that at least three shells are needed to obtain a good agreement between theory and experiment. We underline the need of a third shell to have the first peak (A) on the edge. The use of the HL imaginary potential globally improves the simulation, as shown in Figure 2. In this case, the energy separation and the relative amplitude of the various features are satisfactorily reproduced. A similar analysis was performed on the Cu K-edge of crystalline CuO [15]. For brevity, we report in Figure 3 only the comparison of experimental data and the simulated XANES spectra based on a 6 shells cluster.

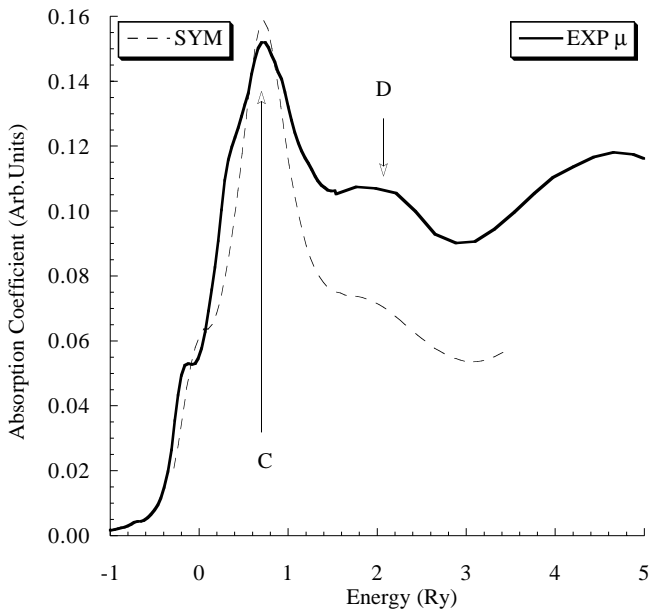


Fig. 3. Comparison between the absorption edge of crystalline CuO and the 6-shell simulation with the HL potential. The local cluster consists in a distorted O octahedron with four atoms at 1.95 Å and two atoms at 2.78 Å, plus four Cu atoms at 2.90 Å, four Cu atoms at 3.08 Å and two Cu atoms at 3.17 Å.

The main features are correctly reproduced at the right energy position, yet small problems remain with the intensity of the white line “C”, which is overestimated. The “D” feature in Figure 3 strongly depends on the number of shells considered in the calculation: to get an appreciable intensity we needed at least 3 shells around the absorber. With 6 shells, a quite good agreement is achieved, as shown in Figure 3.

Turning the attention to the glasses, the simulations were first performed by using a cluster of only nearest neighbors, using data found in previous EXAFS investigations [16–18]. These theoretical calculations did not reproduce all the structures present in the experimental data as in the case of crystalline samples (see Fig. 1 for Cu_2O), evidencing the necessity to include in the simulations contributions coming from further shells. To simulate the glass XANES spectra, geometrical details beyond the first shell were derived from model compounds consisting of silicate glasses with the basic features of the characteristic continuous random network (CRN) of silica [19], and sodium-silicate glasses [20]. For clarity, we separate in two sections the analyses of Cu^{2+} and Cu^+ cases.

3.1 Cu^{2+} in glass

In this section, we will consider only the IG sample. It is expected that in ion implanted samples the local order around Cu strongly depends on the preparation conditions. From our previous EXAFS [16] investigation on implanted soda-lime glasses at either high (5×10^{16} Cu/cm^2) or low (1×10^{16} Cu/cm^2) fluency, we know that in the

latter case only Cu^{2+} ions are present. The first coordination shell around Cu^{2+} ions was found to be formed by $4.0 (\pm 0.5)$ O atoms at $1.87 (\pm 0.02)$ Å; this atomic arrangement is very similar to that of CuO , which consists of four oxygen atoms placed at the corners of an approximately square structure, with a bond length of 1.95 Å [15]. To reproduce the XANES spectra of the IG sample, different model structures have been considered:

- i) In this model, the Cu environment consists of an O square ($\text{Cu}-\text{O} \approx 1.9$ Å) plus 4 Si at 3.2 Å. This kind of environment, based on the structure of synthetic copper sodium silicate $\text{Na}_2\text{Cu}_3(\text{SiO}_2)_4$ [21], was chosen because it does not exhibit Cu–Cu links up to 3.8 Å.
- ii) In this model, beyond the O square, 4 Si and 3 Cu atoms (with a broad distribution of distances between 3.1 and 3.3 Å) was included. This type of structure was chosen on the basis of synthetic (“black”) diopside [22] crystal.
- iii) In this latest model, we considered only a distorted O octahedron made by 4 coplanar atoms at 1.95 Å plus two others at 2.38 Å along the Z -axis, following a model proposed for Cu^{2+} ions 4 mM in water solution [23].

A pictorial view of these clusters is given in Figure 4. The first two structures are based on SiO_4 tetrahedral units linked to the metal and should resemble the local structure around Cu in the glass. In the calculation, we assumed Si–O bond length and angles typical of SiO_4 tetrahedra. Further O atoms were not included due to the highly disordered environment of the glass. All simulations are shown and compared with the experimental spectrum in Figure 5: it can be noted that the main features of the experimental spectrum are present in all the simulations. Namely, feature “E” was obtained in the simulations based solely on the O square only by applying strong (and unphysical) distortions of the first shell environment. This demonstrates that further shells are necessary to reproduce all the features of the spectrum at the right relative energy positions. To a closer inspection, it is clear that models i) and ii) follow the behavior of the experimental spectrum better than model iii), where feature “F” is absent. Therefore, we conclude that further coordination shells do contribute to the shape of the edge and that a Cu–Cu coordination is probably present in the Cu^{2+} sample.

3.2 Cu^+ ions in glass

We considered samples E and IS. The presence of Cu^+ ions in copper-implanted pure silica and soda-lime matrices was evidenced by X-ray photoelectron spectroscopy (XPS) [24] and XAS [16, 18, 25]. From previous XAS investigations [17], we know that in ion-exchanged glass Cu ions are mainly in the Cu^+ oxidation state and are coordinated with $2.0 (\pm 0.7)$ oxygens at a distance $R_{\text{Cu}-\text{O}} = 1.85 (\pm 0.04)$ Å. In the implanted sample, a faint signal from Cu clusters was evidenced together with the presence of an oxide phase with 2 ± 1 O atoms around Cu at

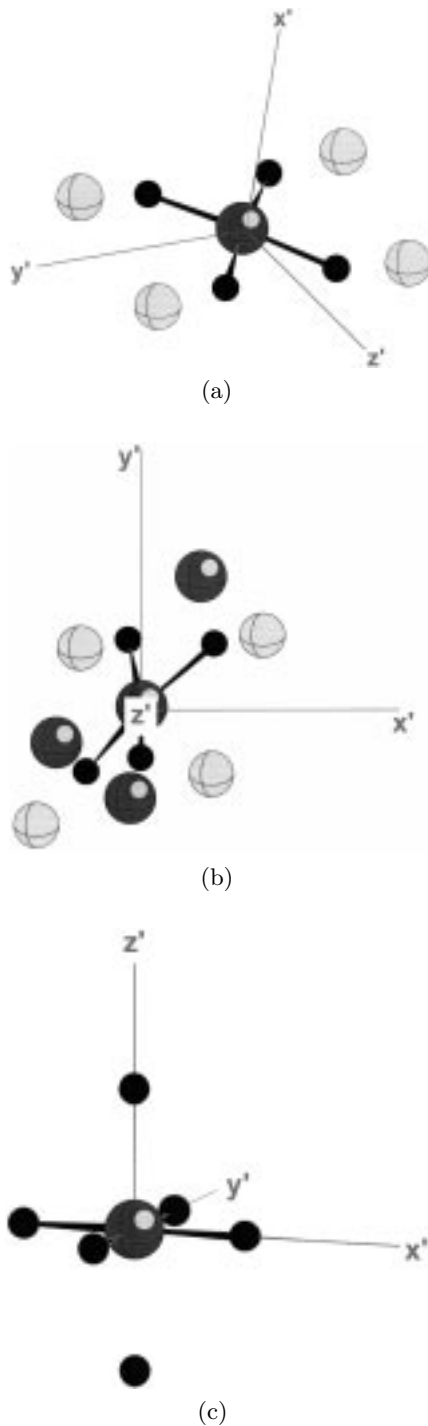


Fig. 4. Pictorial views of the clusters i) (a), ii) (b), and iii) (c) considered in the simulations relative to Cu^{2+} ions. Atoms are indicated with different symbols: Cu (shaded symbol), O (small black symbol) and Si (open symbol).

$1.87 \pm 0.04 \text{ \AA}$ [18]. As for the other case study, a multi-shell method was used to reproduce the absorption edge of the E ad IS samples. In this case, however, no details on the further coordination shells were known. It is worth to stress that is not trivial to find a model compound to start with, since all known Cu silicates reported in literature are based on Cu^{2+} ions. At this purpose, we considered a

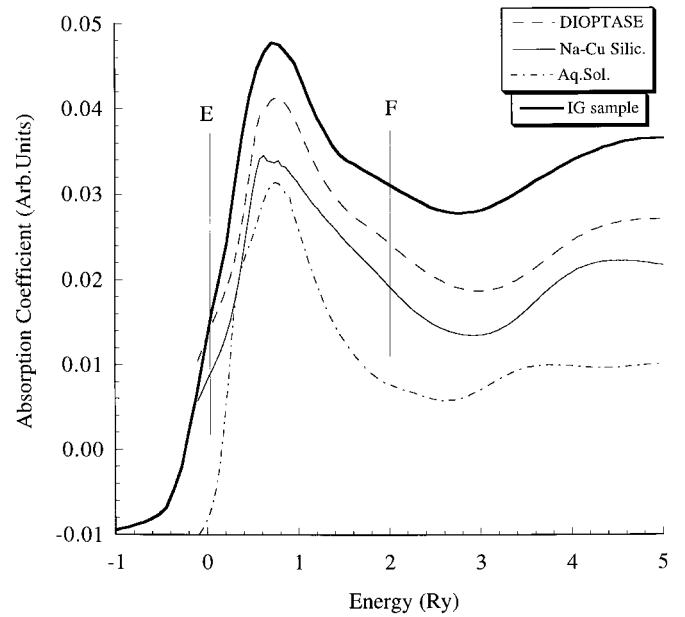


Fig. 5. Comparison among the absorption edge of the IG sample and the simulations of a series of Cu^{2+} compounds. Calculation was performed with the HL potential on local clusters (2-3 shells) taken from the known structures of “black” diop-tase, $\text{Na}_2\text{Cu}_3(\text{SiO}_2)_4$, and from a literature model for Cu^{2+} in aqueous solution.

Table 1. Details on the local clusters used for the simulation of the edge in the case of Cu^+ ions in glass. Structures are derived from a model for Cu^+ ions in Y-Zeolite.

Shell N°	Struct. i)	Struct. i)	Struct. ii)	Struct. ii)
	Radius (\AA)	N^{atoms} , type	Radius (\AA)	N^{atoms} , type
1	1.88	2 O	1.90	3 O
2	2.93	4 Si	2.82	6 Si
3	3.11	2 Si	–	–

Y-zeolite doped with Cu^+ ions. This material was the object of XAS [26] and X-ray powder diffraction [27] studies that determined the chemical state of the metal ions and the details of their local atomic structure. From this structure, a couple of 3-shell models were taken into account for the simulation (see Tab. 1 and Fig. 6):

- i) Two linearly coordinated O plus a double shell of six Si. To check the presence of Cu–Cu coordination in second shell, a second simulation with the outer Si atoms substituted by Cu ones was also performed on this model.
- ii) A Cu–O₃ triangle with an outer shell of six Si.

Assuming model i), the simulations (see Fig. 7) show that the chemical species of the outer atoms strongly modifies the intensity of the “A” peak. In particular, assuming the presence of Cu atoms in a similar environment, the complete cancellation of peak A occurs. So we can conclude that no relevant Cu–Cu interaction is present, in agreement with the EXAFS results. On the other hand (see

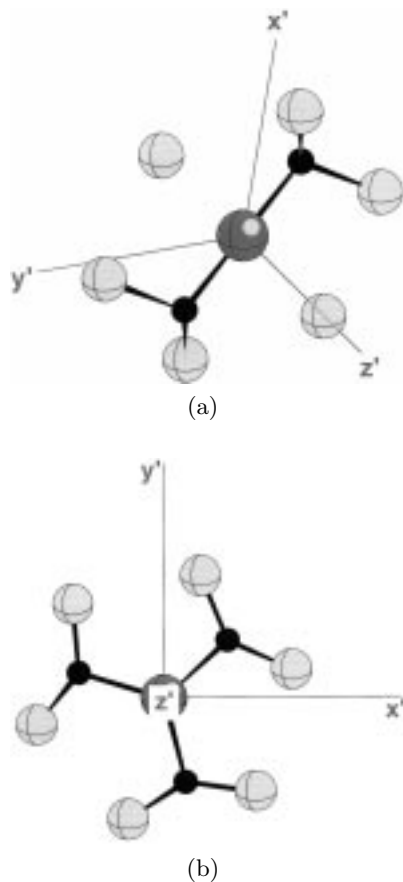


Fig. 6. Pictorial views of the clusters i) (a), and ii) (b) considered in the simulations relative to Cu^+ ions. Atoms are indicated with different symbols: Cu (shaded symbol), O (small black symbol) and Si (open symbol).

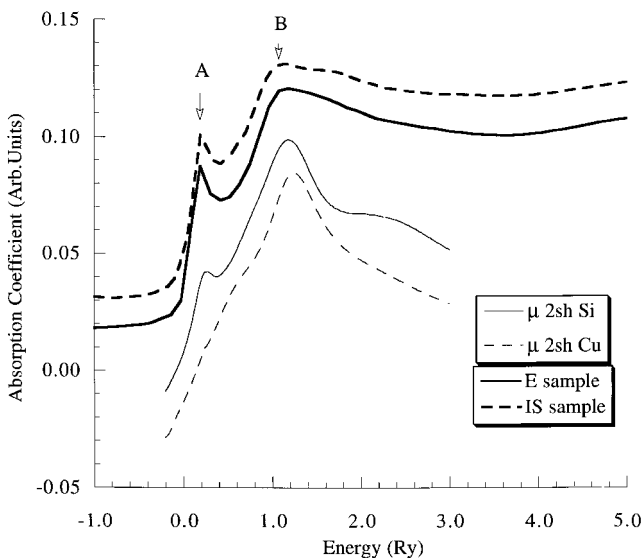


Fig. 7. Comparison of the experimental spectra of Cu^+ samples with the simulations of structure i) (see text). Calculation was performed with different atoms (Cu or Si) in the outer shells.

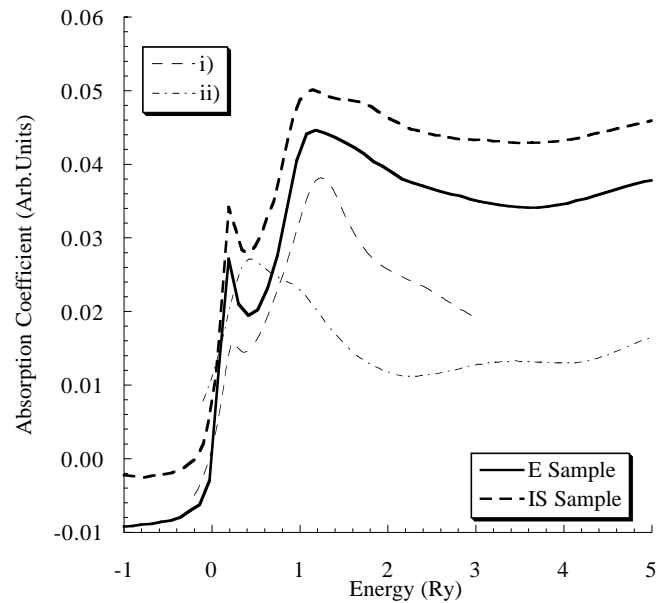


Fig. 8. Comparison among the experimental spectra for Cu^+ ions in glass and calculations. i) and ii) curves are relative to the structures indicated in the text.

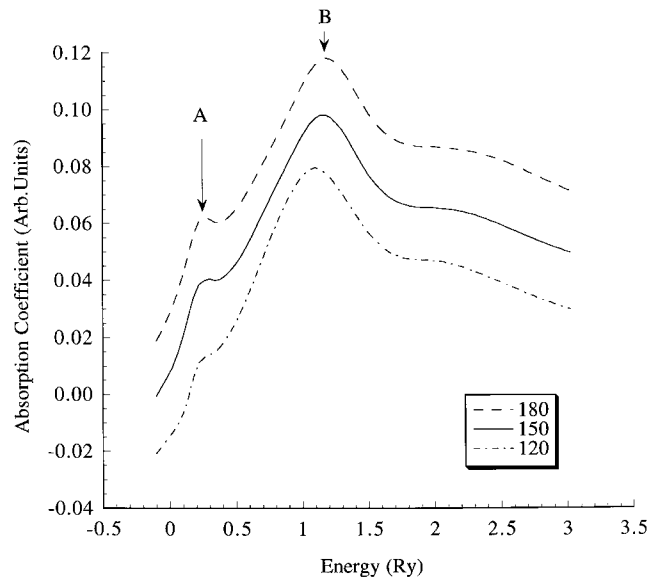


Fig. 9. Simulations of the edge for Cu^+ ions in glass based on structure I and obtained by tilting the O–Cu–O angle from 180° to 120° .

Fig. 8), the “triangle” ii) model behaves quite poorly with these data, leading to a red-shift of the white line without structures on the edge, so we exclude such kind of Cu coordination.

Finally, we looked for the possibility of having a bent O–Cu–O configuration in the framework of model i). Figure 9 shows that changing the O–Cu–O angle from 180 to 120° , while fixing the outer shell configuration, the “A” peak intensity monotonically decreases. This means that the local structure around Cu^+ ions is characterized

by a linear arrangement of the two first neighbors oxygen atoms about the central Cu.

4 Conclusion

In this work, the geometry of the local structures around Cu^+ and Cu^{2+} ions in glass was determined. The analysis of the X-ray absorption coefficient in the near-edge zone evidenced a square local symmetry around Cu^{2+} ions, and a linear coordination of O atoms arounds Cu^+ ions. We can exclude the existence of bent $\text{O}-\text{Cu}^+-\text{O}$ chains or pyramidal arrangements of O around Cu^+ . The introduction of outer coordination shells in the calculation greatly improves the agreement with experimental data. The composition of the outer shells cannot be determined in the Cu^{2+} case, therefore, metal-metal coordination in the second shell cannot be excluded, while for the Cu^+ case the presence of metals can be ruled out.

GILDA is an Italian Collaborating Research Group beamline at the European Synchrotron Radiation Facility ESRF financed by the Italian Institutions CNR, INFM and INFN. The authors are grateful to Dr C. Lamberti for the stimulating discussions.

References

1. R.V. Ramaswamy, R. Srivastava, *IEEE J. Lightwave Technol.* **6**, 984 (1988).
2. P. Mazzoldi, G.W. Arnold, G. Battaglin, F. Gonella, R.F. Haglund Jr., *J. Nonlin. Opt. Phys. Mater.* **5**, 285 (1996).
3. W. Nie, *Adv. Mater.* **5**, 520 (1993).
4. R. Debnath, *J. Lumin.* **43**, 375 (1989).
5. R. Debnath, S.K. Das, *Chem. Phys. Lett.* **155**, 52 (1989).
6. A. Bianconi, in *X-Ray Absorption*, edited by D.C. Königsberger, R. Prins (Wiley, New York, 1988).
7. S. Pascarelli, F. Boscherini, F. d'Acapito, J. Hrdy, C. Meneghini, S. Mobilio, *J. Synchr. Rad.* **3**, 147 (1996).
8. A.F. Wells, *Structural Inorganic Chemistry* (Clarendon, Oxford, 1975).
9. R.N.G. Wyckoff, *Crystal Structures* (Wiley, New York, 1964).
10. L.S. Kau, D.J. Spira-Solomon, J.E. Penner-Hahn, K.O. Hodgson, E.I. Solomon, *J. Am. Chem. Soc.* **109**, 6433 (1987).
11. C.R. Natoli, M. Benfatto, *J. Phys. Colloq. France* **47**, C8 (1986).
12. T.A. Tyson, K.O. Hodgson, C.R. Natoli, M. Benfatto, *Phys. Rev. B* **46**, 5997 (1992).
13. J.G. Norman, *Mol. Phys.* **81**, 1191 (1974).
14. M.O. Krause, J.H. Oliver, *J. Phys. Chem. Ref. Data* **8**, 329 (1979).
15. S. Åsbrink, L.J. Norrby, *Acta Cryst. B* **26**, 8 (1970).
16. F. d'Acapito, S. Mobilio, J.R. Regnard, E. Cattaruzza, F. Gonella, P. Mazzoldi, *J. Non-Cryst. Solids* **232-234**, 364 (1998).
17. F. d'Acapito, S. Colonna, S. Mobilio, F. Gonella, E. Cattaruzza, P. Mazzoldi, *Appl. Phys. Lett.* **71**, 2611 (1997).
18. F. d'Acapito, Ph.D. thesis, University J. Fourier of Grenoble, 1997.
19. R.L. Mozzi, B.E. Warren, *J. Appl. Cryst.* **2**, 164 (1969).
20. G.N. Greaves, A. Fontaine, P. Lagarde, D. Raoux, S.J. Gurman, *Nature* **293**, 611 (1981).
21. K. Kawamura, A. Kawahara, *Acta Cryst. B* **32**, 2419 (1976).
22. K.H. Breuer, W. Eysel, R. Müller, *Z. Kristall.* **187**, 15 (1989).
23. G. Onori, A. Santucci, A. Scafati, M. Belli, S. della Longa, A. Bianconi, L. Palladino, *Chem. Phys. Lett.* **149**, 289 (1988).
24. R. Bertonecello, F. Trivillin, E. Cattaruzza, P. Mazzoldi, G.W. Arnold, G. Battaglin, M. Catalano, *J. Appl. Phys.* **377**, 1294 (1995).
25. K. Fukumi, A. Chayahara, K. Kadono, H. Kageyama, T. Akai, N. Kitamura, M. Makihara, K. Fujii, J. Hayakawa, *J. Non-Cryst. Solids* **238**, 143 (1998).
26. C. Lamberti, G. Spoto, D. Scarano, C. Pazé, M. Salvalaggio, S. Bordiga, A. Zecchina, G. Turnes-Palomino, F. d'Acapito, *Chem. Phys. Lett.* **269**, 500 (1997).
27. C. Lamberti, G.L. Marra, S. Bordiga, A. Zecchina, A. Fitch (in preparation).